PROCEEDINGS OF SCIENCE

Nucleosynthetic Yields from "Collapsars"

Gabriel Rockefeller*[ab], Christopher L. Fryer[ab], Patrick Young[ac], Michael Bennett[ad], Steven Diehl[aeb], Falk Herwig[ad f], Raphael Hirschi[adg], Aimee Hungerford[ab], Marco Pignatari[adh], Georgios Magkotsios[ahc], and Francis X. Timmes[ac]

[a] *The NuGrid Collaboration*
[b] *Computational Physics and Methods (CCS-2), Los Alamos National Laboratory, Los Alamos, NM 87545, USA*
[c] *School of Earth and Space Exploration, Arizona State University, Tempe, AZ 85287, USA*
[d] *Astrophysics Group, Keele University, ST5 5BG, UK*
[e] *Theoretical Astrophysics (T-6), Los Alamos National Laboratory, Los Alamos, NM 87545, USA*
[f] *Dept. of Physics & Astronomy, Victoria, BC, V8W 3P6, Canada*
[g] *IPMU, University of Tokyo, Kashiwa, Chiba 277-8582, Japan*
[h] *Joint Institute for Nuclear Astrophysics, University of Notre Dame, Notre Dame, IN 46556, USA*
E-mail: gaber@lanl.gov

The "collapsar" engine for gamma-ray bursts invokes as its energy source the failure of a normal supernova and the formation of a black hole. Here we present the results of the first three-dimensional simulation of the collapse of a massive star down to a black hole, including the subsequent accretion and explosion. The explosion differs significantly from the axisymmetric scenario obtained in two-dimensional simulations; this has important consequences for the nucleosynthetic yields. We compare the nucleosynthetic yields to those of hypernovae. Calculating yields from three-dimensional explosions requires new strategies in post-process nucleosynthesis; we discuss NuGrid's plan for three-dimensional yields.

10th Symposium on Nuclei in the Cosmos
July 27 - August 1 2008
Mackinac Island, Michigan, USA

*Speaker.

© Copyright owned by the author(s) under the terms of the Creative Commons Attribution-NonCommercial-ShareAlike Licence.

PoS(NIC X)119

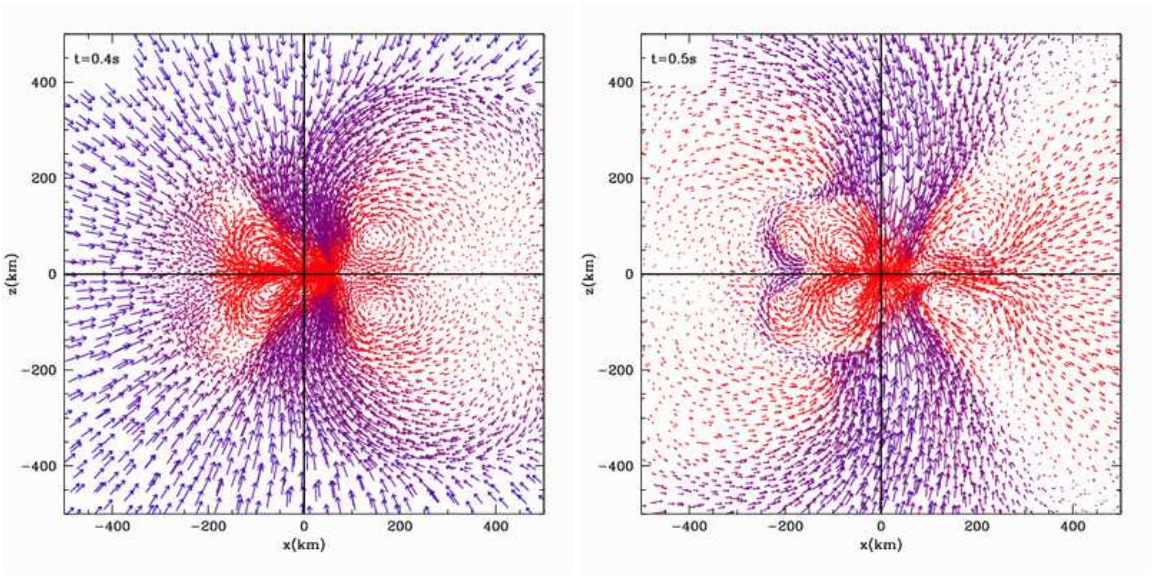

Figure 1: Two slices through the x-z plane of a three-dimensional collapsar calculation. Convection along the plane of rotation, driven by viscous heating from angular momentum transport, ultimately drives a strong explosion. Although the explosion is hypernova-like in energy, it does not have the bipolar asymmetry that we have assumed for collapsars.

1. Explosions from the Collapse of Massive Stars

Woosley [1] argued that a failed supernova could produce an explosion after it collapsed down to a black hole, if the collapsing star were rotating sufficiently rapidly. This model, known as the "collapsar" model, has become the standard model for long-duration gamma-ray bursts; it invokes a magnetic dynamo in the black hole accretion disk [2, 3] to power a relativistic jet and an energetic stellar explosion, referred to as a hypernova.

But what happens if the magnetic dynamo does not work? Although two-dimensional simulations showed that clean disks developed, which were ideal for the formation of gamma-ray burst jets [4, 5], theory predicted a much more chaotic system. In the first three-dimensional simulations of the evolution of a collapsar, we have found that instabilities in the disk lead to matter ejection and hypernova-like explosions [6]. These explosions differ significantly from the jet-driven explosions that Woosley first envisioned. Figure 1 shows two slices (at 0.4 s and 0.5 s after collapse) through the x-z plane from one such simulation (where the z axis is also the axis of rotation of the star) [6]. The progenitor of this explosion is a $60\,M_\odot$ star evolved at zero metallicity, so it experienced low mass loss; the final fate of such a star would be similar even at metallicities as high as 1/100th solar. The star collapses to a black hole, and a disk forms from the fast-rotating silicon layer. Viscous heating drives convection and ultimately an explosion.

2. Yields from Collapsars

Without mass loss, $60\,M_\odot$ stars are believed to collapse directly to black holes [7]. The possible outcomes of this scenario cover a wide range of explosion energies and yields. In the limit

PoS(NIC X)119

Species	Yields ($M_\odot$)			
	Rock1 [6]	Tom50A [8]	Tom50B [8]	CL35 [9]
^{40}Ca	4.07E-02	1.87E-02	1.20E-02	1.70E-02
^{41}Ca	3.80E-07	1.72E-06	4.78E-07	2.07E-06
^{42}Ca	2.85E-06	2.29E-07	7.46E-08	1.54E-06
^{43}Ca	3.88E-09	7.31E-07	4.75E-07	1.56E-09
^{44}Ca	5.86E-08	6.08E-04	3.95E-04	1.03E-05
^{45}Ca	4.20E-09	-	-	7.22E-14
^{46}Ca	4.21E-08	2.66E-13	6.72E-14	3.96E-15
^{47}Ca	1.56E-09	-	-	-
^{48}Ca	1.35E-04	1.56E-13	6.72E-14	2.13E-19
^{45}Sc	5.04E-08	6.31E-08	3.69E-08	1.05E-07
^{44}Ti	9.23E-05	6.08E-04	3.95E-04	1.03E-05
^{46}Ti	8.86E-06	1.40E-05	9.07E-06	1.02E-06
^{47}Ti	4.89E-08	5.85E-05	3.80E-05	4.13E-08
^{48}Ti	9.09E-08	7.84E-04	5.09E-04	1.94E-04
^{49}Ti	9.86E-08	3.93E-06	2.55E-06	8.86E-06
^{50}Ti	2.93E-05	1.45E-12	5.46E-13	1.89E-13
^{50}V	6.42E-08	1.14E-12	2.83E-13	6.60E-12
^{51}V	5.06E-07	7.13E-05	4.63E-05	1.06E-05
^{50}Cr	3.12E-05	9.36E-06	6.06E-06	1.35E-05
^{52}Cr	1.78E-05	3.13E-03	2.03E-03	3.43E-03
^{53}Cr	1.21E-06	4.87E-05	3.15E-05	2.00E-04
^{54}Cr	6.28E-05	6.61E-12	1.72E-12	2.15E-10
^{55}Mn	1.42E-06	2.87E-05	1.86E-05	5.89E-04
^{54}Fe	4.35E-04	2.51E-05	1.63E-05	1.59E-03
^{56}Fe	7.15E-05	3.61E-01	2.34E-01	1.00E-01
^{57}Fe	3.47E-06	7.35E-03	4.77E-03	1.07E-03
^{58}Fe	1.68E-04	1.53E-11	4.52E-12	1.34E-10
^{60}Fe	1.04E-04	1.11E-12	3.86E-13	1.31E-21
^{59}Co	6.58E-07	1.34E-03	8.70E-04	7.58E-06
^{60}Co	4.64E-08	-	-	2.86E-16
^{56}Ni	4.74E-02	3.61E-01	2.34E-01	1.00E-01
^{57}Ni	4.55E-04	7.35E-03	4.77E-03	1.02E-03
^{58}Ni	2.32E-02	2.76E-03	1.79E-03	3.24E-04
^{60}Ni	2.42E-03	1.31E-02	8.49E-03	3.06E-04
^{61}Ni	4.43E-06	2.18E-04	1.42E-04	6.29E-06
^{62}Ni	9.44E-04	1.43E-04	9.31E-05	7.66E-06
^{64}Ni	4.93E-04	6.72E-12	1.67E-12	2.12E-15

Table 1: Yields from our explosion of a $60\,M_\odot$ star compared to other low-metallicity calculations in the literature: two $50\,M_\odot$ stars [8] and a $35\,M_\odot$ star [9]. The $50\,M_\odot$ and $35\,M_\odot$ stars differentiate between stable isotopes (that include the decay products into that isotope) whereas our explosion is the yield at the time of the explosion.

PoS(NIC X)119

where the progenitor star is non-rotating, such a collapse would produce no explosion whatsoever. At the other extreme, the collapse of a rotating star could produce a hypernova [8]. The nucleosynthetic yields of these hypernovae are not too different from the yields from standard nuclear yield studies [9]. In this section, we compare the yields from our three-dimensional simulation to those of hypernovae and "standard-yield" explosions (table 1).

To carry out our three-dimensional simulation, we used the SNSPH code [10] to model the evolution of over 2.5 million smooth particle hydrodynamics (SPH) points covering the entire star. For this paper, we consider only the $\sim 250,000$ particles that burned into iron-peak elements. The Lagrangian nature of SPH allows us to easily extract the density and temperature evolution of each particle as a function of time. We apply a post-process burning code to each of these particles to obtain its nucleosynthetic yield using a 524-element network [11].

The results in table 1 show that our explosion produced considerably less ^{56}Ni than either the hypernova calculations [8] or the standard-yield explosions [9]. Our explosion is slightly less energetic than the hypernova explosions, so the difference from the hypernova results is not too surprising. However, the fact that we do not produce as much ^{56}Ni as the standard nucleosynthetic yield calculations highlights one of the major issues with these older yield results. Models using piston-driven explosions artificially eject matter by neglecting fallback [12], which leads to overproduction of ^{56}Ni. In addition, standard nucleosynthetic yield calculations are driving explosions in massive stars (i.e., stars above $20\,M_\odot$) that can only be expected in rapidly-rotating models such as our collapsars or in hypernovae. One of NuGrid's goals is to determine the effect such assumptions have on the integrated yields.

There is a wealth of information in table 1, but here we mention only a few other features. The hypernova calculations produce more ^{44}Ti than our explosion; this is likely due to the larger mass of high-entropy material produced in the more focused jet explosion. At high neutron number, the amounts of elements in the hypernova and standard supernova explosions drop dramatically; this is probably an artifact of the smaller nuclear networks used in those calculations. At the edges of networks, the yields are not very reliable. Our larger network produces more of these isotopes.

3. Implications

Will such explosions be observable? Will their yields contribute noticeably to the abundances of isotopes in the universe? These explosions will only occur in low-metallicity stars (i.e., stars with metallicities less than 1/100th solar). Figure 2 shows the fraction of stars formed that have such low metallicities as a function of redshift. Below a redshift of 2.8, very few stars have sufficiently low metallicities to produce the explosions we observe. This high redshift limit, coupled to our low simulated ^{56}Ni abundance (a large ^{56}Ni abundance is very helpful in producing bright light-curves), means that this type of explosion will not be detected by any upcoming telescopes. The lower yields from this explosion, compared to earlier "standard-yield" simulations, imply that massive stars have even less impact on the global abundance pattern than has been previously thought.

The differences in the yields can be attributed to a number of effects: different explosion mechanisms, different progenitors, and different nuclear networks (interestingly, network uncertainties are probably bigger than rate uncertainties at this point in time). Our NuGrid collaboration is studying each of these effects systematically to reduce errors and to present a set of results in-

PoS(NIC X)119

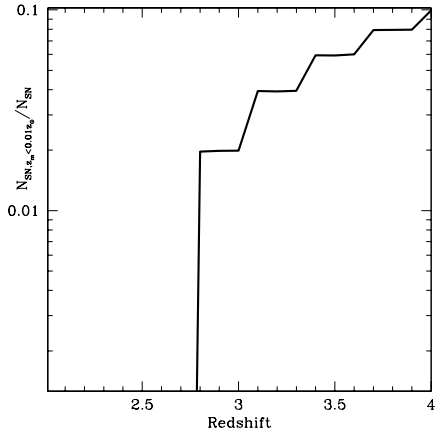

Figure 2: Fraction of stars with metallicities below $0.01Z_\odot$ (a requirement for the direct collapse of $60\,M_\odot$ stars to black holes) as a function of redshift. The fraction drops off precipitously at a redshift of 2.8, so we do not expect the explosions simulated here to occur at lower redshifts.

cluding error bars caused by current uncertainties. We have also revised how we manage data, introducing new data formats to deal will > 1 million particle simulations.

References

[1] S. E. Woosley 1993, *Gamma-ray bursts from stellar mass accretion disks around black holes*, ApJ, **405**, 273

[2] R. Narayan, B. Paczynski, T. Piran 1992, *Gamma-ray bursts as the death throes of massive binary stars*, ApJ, **395**, L83

[3] R. Popham, S. E. Woosley, C. Fryer 1999, *Hyperaccreting Black Holes and Gamma-Ray Bursts*, ApJ, **518**, 356

[4] A. I. MacFadyen, S. E. Woosley 1999, *Collapsars: Gamma-Ray Bursts and Explosions in "Failed Supernovae"*, ApJ, **524**, 262

[5] D. Proga, A. I. MacFadyen, P. J. Armitage, M. C. Begelman 2003, *Axisymmetric Magnetohydrodynamic Simulations of the Collapsar Model for Gamma-Ray Bursts*, ApJ, **599**, L5

[6] G. Rockefeller, C. L. Fryer, H. Li 2008, *Collapsars in Three Dimensions*, astro-ph/0608028

[7] C. L. Fryer 1999, *Mass Limits for Black Hole Formation*, ApJ, **522**, 413

[8] N. Tominaga, H. Umeda, K. Nomoto 2007, *Supernova Nucleosynthesis in Population III 13-15 $M_{\rm solar}$ Stars and Abundance Patterns of Extremely Metal-poor Stars*, ApJ, **660**, 516

[9] A. Chieffi, M. Limongi 2004, *Explosive Yields of Massive Stars from Z=0 to Z=$Z_\odot$*, ApJ, **608**, 405

[10] C. L. Fryer, G. Rockefeller, M. S. Warren 2006, *SNSPH: A Parallel Three-dimensional Smoothed Particle Radiation Hydrodynamics Code*, ApJ, **643**, 292

[11] P. A. Young, C. L. Fryer, A. Hungerford, D. Arnett, G. Rockefeller, F. X. Timmes, B. Voit, C. Meakin, K. A. Eriksen 2006, *Constraints on the Progenitor of Cassiopeia A*, ApJ, **640**, 891

[12] P. A. Young, C. L. Fryer 2007, *Uncertainties in Supernova Yields. I. One-Dimensional Explosions*, ApJ, **664**, 1033

PoS(NIC X)119